

# Critical velocity of superfluid flow through single barrier and periodic potentials

Gentaro Watanabe,<sup>1,2</sup> F. Dalfovo,<sup>1</sup> F. Piazza,<sup>1</sup> L. P. Pitaevskii,<sup>1,3</sup> and S. Stringari<sup>1</sup>

<sup>1</sup>*CNR INFM-BEC and Department of Physics, University of Trento, 38050 Povo, Italy*

<sup>2</sup>*RIKEN, 2-1 Hirosawa, Wako, Saitama 351-0198, Japan*

<sup>3</sup>*Kapitza Institute for Physical Problems, 119334 Moscow, Russia*

(Dated: July 2, 2009)

We investigate the problem of an ultracold atomic gas in the superfluid phase flowing in the presence of a potential barrier or a periodic potential. We use a hydrodynamic scheme in the local density approximation (LDA) to obtain an analytic expression for the critical current as a function of the barrier height or the lattice intensity, which applies to both Bose and Fermi superfluids. In this scheme, the stationary flow becomes energetically unstable when the local superfluid velocity is equal to the local sound velocity at the point where the external potential is maximum. We compare this prediction with the results of the numerical solutions of the Gross-Pitaevskii and Bogoliubov-de Gennes equations. We discuss the role of long wavelength excitations in determining the critical velocity. Our results allow one to identify the different regimes of superfluid flow, namely, the LDA hydrodynamic regime, the regime of quantum effects beyond LDA for weak barriers and the regime of tunneling between weakly coupled superfluids for strong barriers. We finally discuss the relevance of these results in the context of current experiments with ultracold gases.

PACS numbers: 03.75.Lm, 03.75.Ss

## I. INTRODUCTION

The critical velocity of superfluid flow is one of the most fundamental issues in the physics of quantum fluids. A mechanism for the onset of dissipation is provided by Landau instability [1, 2, 3, 4]: if the excitation spectrum satisfies suitable criteria, there exists a critical flow velocity above which the kinetic energy of the superfluid can be dissipated *via* the creation of excitations. For uniform weakly interacting Bose gases, this critical velocity  $v_c$  coincides with the velocity of sound waves. Several experiments have already been devoted to observe and characterize the onset of dissipation in superfluids made of ultracold atomic gases, including studies of Bose-Einstein condensates (BECs) in relative motion with respect to external perturbations, such as point-like defects [5] or weak optical lattices [6].

The present work was stimulated by the recent experiment by Miller *et al.* [7], where a one-dimensional (1D) optical lattice is used to measure the critical velocity of the superfluid flow of ultracold fermionic atoms in the BCS-BEC crossover. The lattice is produced by two intersecting laser beams focused in the central part of the trapped gas. A frequency difference between the two beams is used to produce a relative motion of the lattice and the gas. The number of fermion pairs which remain in the superfluid after the application of the moving lattice is measured as a function of the relative velocity in order to determine the critical velocity for the onset of dissipation. The experiment confirms a theoretical prediction that superfluidity is most robust at unitarity [8, 9, 10]. It also shows that the critical velocity is very sensitive to the intensity of the lattice. This shares some similarity with the flow of a superfluid in the presence of a single potential barrier. In the case of

ultracold fermions in the BCS-BEC crossover, the latter problem has been recently addressed in the framework of the Bogoliubov-de Gennes (BdG) theory by Spuntarelli *et al.* [11], who also found a strong dependence of the critical velocity on the barrier height. These works (see also, e.g., Refs. [12, 13, 14, 15, 16]) are recent fermionic examples of a wider field of investigations of critical current phenomena mainly studied, in the past, for Bose-Einstein condensed gases. We notice however that the similarities and differences between the behavior of the critical flow in the presence of a single barrier and of a periodic potential, as well as the role of quantum statistics have never been addressed in a clear and systematic way.

Our work is aimed to establish an appropriate framework where one can compare the different situations (bosons vs. fermions and single barrier vs. optical lattice) and extract useful indications for available and/or feasible experiments. To this purpose we first introduce the hydrodynamic formalism in the local density approximation (LDA) and we assume a polytropic equation of state, which applies both to a Fermi superfluid at unitarity (i.e., when the  $s$ -wave scattering length  $a_s$  is much larger than the interparticle distance, which in turn is much larger than the range of the interatomic potential) and to a Bose-Einstein condensate. In this way we derive a universal relation between the critical current for energetic instability and the maximum value of the external potential. We then compare the LDA hydrodynamic prediction with the results of the numerical solutions of the Gross-Pitaevskii (GP) and Bogoliubov-de Gennes equations for bosons and fermions, respectively. This comparison allows us to identify different regimes of superfluid flow depending on the relevant energy and length scales of the system: a regime of hydrodynamic flow in LDA, a

regime of macroscopic flow beyond LDA, and a regime of weakly coupled superfluids separated by thin and strong barriers. From our analysis one can see that the BdG results of Ref. [11] for fermions at unitarity nicely fall into the LDA hydrodynamic regime. Conversely, the parameters of the experiment in Ref. [7] are such that the LDA is not applicable, the healing length being of the same order of the lattice spacing. Indeed we find that the experimental results are not reproduced by the LDA, as expected, but we find that they also disagree with the BdG theory in a periodic potential with parameters similar to the ones of the experiment. This disagreement suggests that the interpretation of the experimental observations in terms of energetic instability of stationary superfluid flow in a uniform 1D periodic potential remains an open issue.

## II. HYDRODYNAMICS IN THE LOCAL DENSITY APPROXIMATION

Our starting point is a hydrodynamic theory in the local density approximation at zero temperature. Let us consider a superfluid which extends to infinity in three dimensions and is subject to a 1D potential,  $V_{\text{ext}}(z)$ , which has a finite maximum value  $V_{\text{max}}$ . Let the superfluid be in a stationary configuration characterized by the density profile  $n(z)$  and the (quasi-) momentum  $P(z)$  along the  $z$ -direction. The LDA assumes that, locally, the system behaves like a uniform gas; thus the energy density  $e(n, P)$  can be written in the form  $e(n, P) = nP^2/2m + e(n, 0)$  and one can define the local chemical potential  $\mu(n) = \partial e(n, 0)/\partial n$ . The density profile of the gas at rest in the presence of the external potential can be obtained from the Thomas-Fermi relation  $\mu_0 = \mu(n(z)) + V_{\text{ext}}(z)$ . If the gas is flowing with a constant current density  $j = n(z)v(z)$ , the Bernoulli equation for the stationary velocity field  $v(z)$  is

$$\mu_j = \frac{m}{2} \left[ \frac{j}{n(z)} \right]^2 + \mu(n) + V_{\text{ext}}(z), \quad (1)$$

where  $\mu_j$  is the  $z$ -independent value of the chemical potential. This equation gives the density profile, for any given current  $j$ , once the equation of state  $\mu(n)$  of the uniform gas of density  $n$  is known. We assume the uniform gas to obey a polytropic equation of state,  $\mu(n) = \alpha n^\gamma$ , and we consider two cases: i) a dilute Bose gas with repulsive interaction, for which one has  $\gamma = 1$  and  $\alpha = g = 4\pi\hbar^2 a_s/m$ , where  $g$  is the interaction parameter,  $m$  is the atom mass, and  $a_s > 0$  is the  $s$ -wave scattering length; ii) a dilute Fermi gas at unitarity, for which  $\mu(n) = (1 + \beta)E_F$ , where  $\beta$  is a universal parameter [17, 18] while  $E_F = \hbar^2 k_F^2/(2m)$  and  $k_F = (3\pi^2 n)^{1/3}$  are the Fermi energy and momentum, respectively, of a uniform non-interacting Fermi gas of density  $n$ , so that  $\gamma = 2/3$  and  $\alpha = (1 + \beta)(3\pi^2)^{2/3}\hbar^2/(2m)$ . Using the

equation of state one can write

$$mc_s^2(z) = n \frac{\partial}{\partial n} \mu(n) = \gamma \mu(n), \quad (2)$$

where  $c_s(z)$  is the local sound velocity, which depends on  $z$  through the density profile  $n(z)$ . In a uniform gas of density  $n_0$ , the sound velocity is given by  $c_s^{(0)} = [\gamma \mu(n_0)/m]^{1/2}$ .

In the framework of LDA, the system becomes energetically unstable when the local superfluid velocity,  $v(z)$  at some point  $z$  is equal to the local sound velocity,  $c_s(z)$ . If the external potential has a maximum at  $z = z_0$  [i.e.,  $V_{\text{ext}}(z_0) = V_{\text{max}}$ ], then at the same point the density is minimum,  $c_s(z)$  is minimum and  $v(z)$  is maximum. This means that the superfluid becomes first unstable precisely at  $z = z_0$ . The condition for the occurrence of the instability can be written as  $m[j_c/n_c(z_0)]^2 = \gamma \mu[n_c(z_0)] = \gamma \alpha n_c^\gamma(z_0)$ , where  $n_c(z)$  is the density profile calculated at the critical current [19]. By inserting this condition into the Bernoulli equation (1), after a straightforward calculation one obtains the following implicit relation for the critical current:

$$j_c^2 = \frac{\gamma}{m\alpha^{2/\gamma}} \left[ \frac{2\mu_{j_c}}{2 + \gamma} \left( 1 - \frac{V_{\text{max}}}{\mu_{j_c}} \right) \right]^{\frac{2}{\gamma} + 1}. \quad (3)$$

It is worth noticing that this equation contains only  $z$ -independent quantities. It is also independent of the shape of the external potential: the only relevant parameter being its maximum value  $V_{\text{max}}$ . Moreover, it can be applied to both bosons and fermions. Its version for bosons in slowly varying potentials was already discussed in Refs. [20, 21] (see also Ref. [22]).

In Figs. 1 and 2, we plot the critical velocity obtained from the hydrodynamic expression (3) for bosons and fermions, respectively (thick solid lines). The upper plots refer to the case of a single 1D rectangular barrier of width  $L$  and height  $V_{\text{max}}$ , the superfluid having an asymptotic constant density  $n_0$  and velocity  $v_0 \equiv j/n_0$  at large distances from the barrier. The bottom plots refer to the case of a 1D periodic potential  $V_{\text{ext}}(z) = V_{\text{max}} \sin^2(q_B z) = sE_R \sin^2(q_B z)$ , where  $q_B$  is the Bragg wave vector,  $E_R \equiv \hbar^2 q_B^2/2m$  is the recoil energy,  $s$  is the lattice strength, and the superfluid has an average density  $n_0$  and a macroscopic velocity defined by  $v_0 \equiv j/n_0$ . In all cases, the critical velocity  $v_c = j_c/n_0$  is normalized to the value of the sound velocity in the uniform gas,  $c_s^{(0)}$ , and is plotted as a function of  $V_{\text{max}}/\mu_{j=0}$  (see Appendix A). The limit  $V_{\text{max}}/\mu_{j=0} \rightarrow 0$  corresponds to the usual Landau criterion for a uniform superfluid flow in the presence of a small external perturbation, i.e., a critical velocity equal to the sound velocity of the gas. In this hydrodynamic scheme, as mentioned before, the critical velocity decreases when  $V_{\text{max}}$  increases mainly because the density has a local depletion and the velocity has a corresponding local maximum, so that the Landau instability occurs earlier. When  $V_{\text{max}} = \mu_{j_c}$ , the density

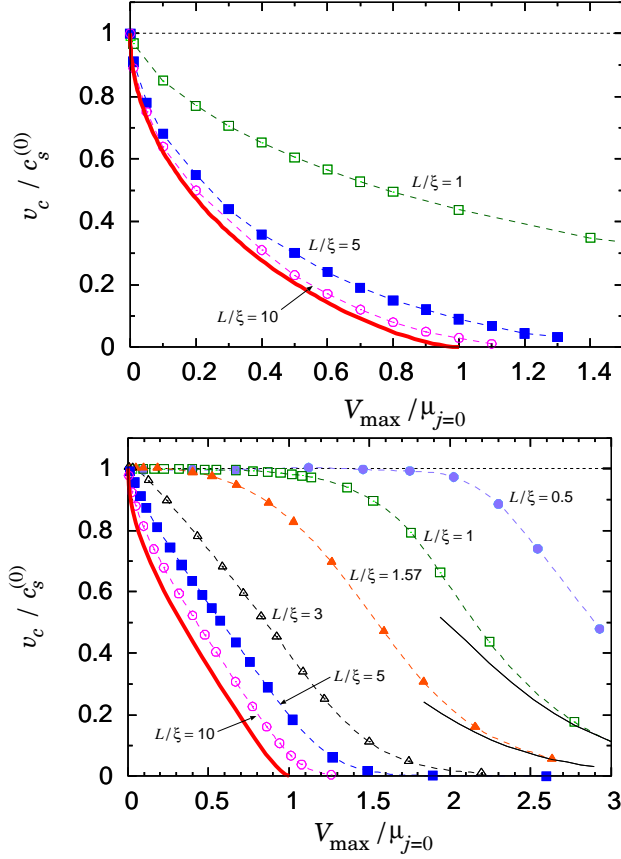


FIG. 1: (Color online) Critical velocity for energetic instability of a dilute bosonic superfluid subject to a 1D external potential. The critical velocity is given in units of the sound velocity of a uniform gas,  $c_s^{(0)}$ , and is plotted as a function of the maximum of the external potential in units of the chemical potential  $\mu_{j=0}$  of the superfluid at rest. Top panel: the case of a single potential barrier. Bottom panel: the case of a periodic potential. Thick solid lines: prediction of the hydrodynamic theory within the LDA, calculated from Eq. (3). Symbols: results obtained from the numerical solution of the GP equation (4) for various values of  $L/\xi$ . Filled circles:  $L/\xi = 0.5$  ( $gn_0/E_R = 0.1$ ); open squares:  $L/\xi = 1$  ( $gn_0/E_R = 0.4$ ); filled triangles:  $L/\xi = 1.57$  ( $gn_0/E_R = 1$ ); open triangles:  $L/\xi = 3$  ( $gn_0/E_R = 3.65$ ); filled squares:  $L/\xi = 5$  ( $gn_0/E_R = 10$ ); open circles:  $L/\xi = 10$  ( $gn_0/E_R = 40$ ). The thinner black solid lines are the tight-binding prediction (9) for  $L/\xi = 1$  and  $1.57$ . Dashed lines are guides to the eye.

exactly vanishes below the barrier and hence the critical velocity goes to zero.

The condition for the applicability of the LDA expression (3) is that the typical length scale of the external potential must be much larger than the healing length  $\xi$  of the superfluid. For a 1D potential barrier of width  $L$ , this implies  $L/\xi \gg 1$  [23]. In an optical lattice, the typical scale is the lattice spacing  $d = \pi/q_B$ ; in order to compare the two cases we define the barrier width  $L$  as half the lattice spacing, i.e.,  $L \equiv d/2 = \pi/(2q_B)$ . The healing length of a dilute Bose superfluid of density  $n_0$  is

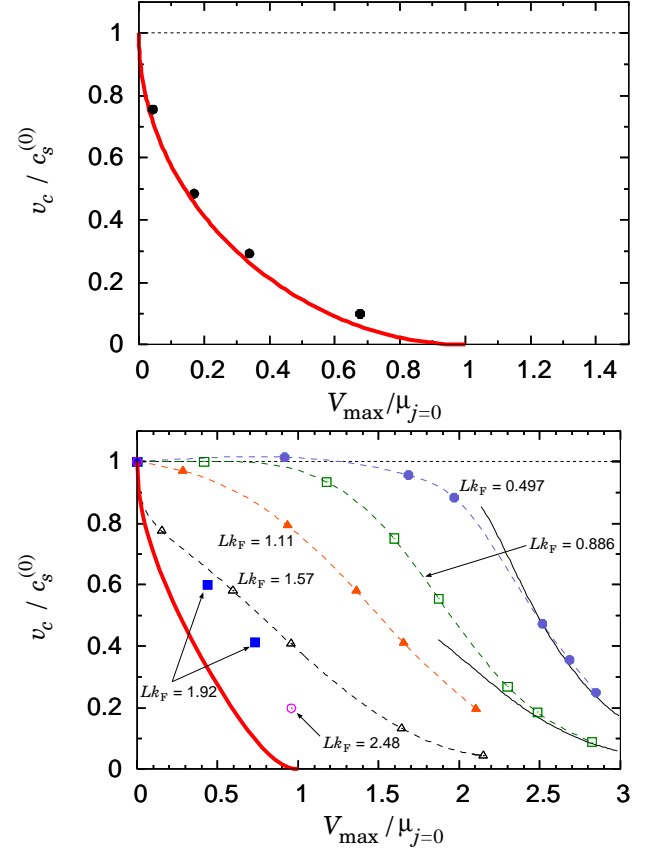


FIG. 2: (Color online) Same as in Fig. 1 but for a superfluid of dilute fermions at unitarity. Thick solid lines: prediction of the LDA hydrodynamic theory, from Eq. (3). Symbols in the top panel: BdG results of Ref. [11] with  $Lk_F = 4$ . Symbols in the bottom panel represent our BdG results for a periodic lattice. The  $s \neq 0$  values are shown as follows: filled circles for  $Lk_F = 0.497$  ( $E_F/E_R = 0.1$ ) and  $s = 0.1, 0.5, 1, 2.5, 3$ , and  $3.5$ ; open squares for  $Lk_F = 0.886$  ( $E_F/E_R = 0.3178$ ) and  $s = 0.1, 0.5, 1, 1.5, 2.5, 3$ , and  $4$ ; filled triangles for  $Lk_F = 1.11$  ( $E_F/E_R = 0.5$ ) and  $s = 0.1, 0.5, 1, 1.5$ , and  $2.5$ ; open triangles for  $Lk_F = 1.57$  ( $E_F/E_R = 1$ ) and  $s = 0.1, 0.5, 1, 2.5$ , and  $4$ ; filled squares for  $Lk_F = 1.92$  ( $E_F/E_R = 1.5$ ) and  $s = 0.5$  and  $1$ ; open circle for  $Lk_F = 2.48$  ( $E_F/E_R = 2.5$ ) and  $s = 2.5$ . The result for  $Lk_F = 0.497$  and  $s = 0.1$  being larger than unity is due to the numerical uncertainty, which is estimated to be of the order of 3% or less for all BdG points in the bottom panel of this figure. The thinner black solid lines are the tight-binding prediction (9) for  $Lk_F = 0.497$  and  $0.886$ . Dashed lines are guides to the eye.

$\xi = \hbar/(2mgn_0)^{1/2}$ , while for a Fermi gas at unitarity one has  $\xi \sim 1/k_F$ , which is consistent with the BCS coherence length  $\xi_{\text{BCS}} = \hbar v_F/\Delta_{\text{gap}}$ , where  $v_F = \hbar k_F/m$  and  $\Delta_{\text{gap}}$  is the pairing gap, which is of order  $E_F$  at unitarity. Effects beyond LDA become important when  $\xi$  is of the same order or larger than  $L$ ; they cause a smoothing of both density and velocity distributions, as well as the emergence of solitonic excitations, which are expected to play an important role in determining the critical veloc-

ity. This is well known for bosons, where a supercritical current results in the emission of shock waves in classical hydrodynamics and of solitons in the Gross-Pitaevskii theory [21, 24, 25].

In closing this section, it is worth mentioning that within the LDA scheme one can easily calculate also the current(velocity)-phase relation of the superfluid flowing through a single potential barrier. The phase  $\phi$  of the order parameter is related to the local velocity by  $v(z) = (\hbar/M)\nabla\phi$ , where  $M = m$  for Bose superfluids and  $M = 2m$  for Fermi superfluids. For a given asymptotic velocity  $v_0 = j/n_0$  at  $z = \pm\infty$ , one can directly integrate the phase across the barrier in order to obtain the phase difference  $\delta\phi$ . By subtracting the contribution of  $v_0$ , the phase difference can be defined as  $\delta\phi \equiv (M/\hbar) \int_{-\infty}^{\infty} dz [v(z) - v_0]$ . In the LDA, the local velocity  $v(z)$  is constant under the rectangular barrier and one thus obtains  $\delta\phi = ML[v(z_0) - v_0]/\hbar$ . Examples are shown in Fig. 3 for bosons with  $L/\xi = 10$  (top panel) and unitary fermions with  $Lk_F = 4$  (bottom panel). The predictions of the hydrodynamic theory within LDA are shown as solid lines for three values of the barrier height. Each line is drawn up to the value of  $\delta\phi_c$  for which the velocity becomes maximum. These lines are called stable branches in the current(velocity)-phase diagram; on the right of the maximum there are no solutions within LDA (see the end of Section III for details). The maximum velocity coincides with the critical velocity  $v_c$  plotted in the top panels of Figs. 1 and 2.

### III. GROSS-PITAEVSKII THEORY FOR BOSONS

In order to account for effects beyond the LDA hydrodynamic theory we use the GP theory for dilute bosons [26, 27, 28] and the BdG equations for fermions at unitarity [29]. Let us first consider the case of a dilute 3D Bose-Einstein condensate at zero temperature subject to either a 1D rectangular potential barrier or a periodic potential. The system is well described by the 1D GP equation [28]:

$$-\frac{\hbar^2}{2m}\partial_z^2\Psi + V_{\text{ext}}(z)\Psi + g|\Psi|^2\Psi = \mu\Psi, \quad (4)$$

where  $\Psi(z) = \sqrt{n(z)}\exp[i\phi(z)]$  is the complex order parameter of the condensate,  $\phi(z)$  is its phase, and  $\mu$  is the chemical potential. The local superfluid velocity is given by  $v(z) = (\hbar/m)\partial_z\phi(z)$  and the sound velocity in a uniform condensate of density  $n_0$  is  $c_s^{(0)} = \sqrt{gn_0/m}$ . We numerically solve the GP equation in order to find the condition for the energetic stability of the condensate.

In the case of a single barrier, we calculate the critical current by looking for solutions of the time-independent GP equation (4) at a fixed current  $j$  and for a given asymptotic density  $n_0$  [30]. We also use the time-dependent version of the GP equation in order to check

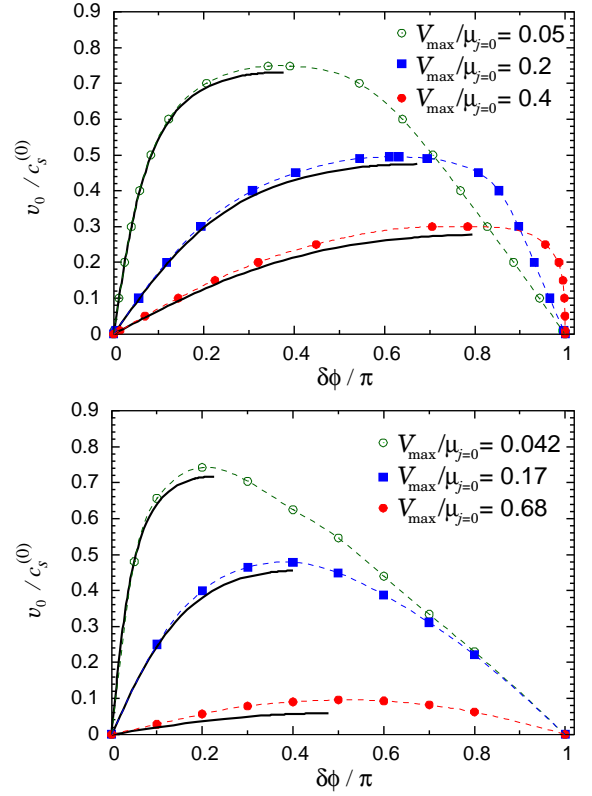


FIG. 3: (Color online) Velocity-phase diagrams in the LDA hydrodynamic regime for a bosonic superfluid (top panel) and for a fermionic superfluid at unitarity (bottom panel) through a single barrier. The thick solid lines show the prediction of the LDA hydrodynamic theory. The symbols in the top panel are the results obtained from the GP equation; those in the bottom panel are taken from the BdG results of Ref. [11]. The barrier heights for bosonic case are  $V_{\text{max}}/\mu_{j=0} = 0.05$  (open circles), 0.2 (filled squares), and 0.4 (filled circles). Those for fermionic case are  $V_{\text{max}}/\mu_{j=0} = 0.042$  (open circles), 0.17 (filled squares), and 0.68 (filled circles). The barrier width is  $L/\xi = 10$  for the bosonic case, and  $Lk_F = 4$  for the fermionic case; these parameters are such that the corresponding curves for  $v_c/c_s^{(0)}$  in the top panels of Figs. 1 and 2 are qualitatively similar. The dashed lines are guides to the eye.

the dynamical behavior of the unstable solutions. In the case of the periodic potential, the critical current is instead found by using the Bloch wave formalism and solving the linear stability problem for the GP energy functional as in Refs. [31, 32, 33]. For the same case, we also use an alternative method, namely, a hydrodynamic analysis of the excitations, which is valid when the excitations that trigger the instability are those with wavelength much larger than the lattice spacing. For a superfluid with average density  $n_0$  and quasi-momentum  $P$ , this approach predicts the dispersion relation

$$\omega(q) = \frac{\partial^2 e}{\partial n_0 \partial P} q + \sqrt{\frac{\partial^2 e}{\partial n_0^2} \frac{\partial^2 e}{\partial P^2}} |q|, \quad (5)$$

where  $\hbar\omega$  and  $q$  are the energy and the wavenumber of the excitations. The energetic instability occurs when [12, 32, 34]

$$\frac{\partial^2 e}{\partial n_0 \partial P} = \sqrt{\frac{\partial^2 e}{\partial n_0^2} \frac{\partial^2 e}{\partial P^2}}. \quad (6)$$

In practice, we calculate the energy density  $e(n_0, P)$  by solving the GP equation for a given average density  $n_0$  and quasi-momentum  $P$  of the superfluid. The value of  $P$  for which Eq. (6) is satisfied is the critical quasi-momentum,  $P_c$ . Finally, the critical velocity can be calculated by using the relation  $v_c = (1/n_0)(\partial e/\partial P)_{P_c}$  (see Appendix B for details). We have checked that the critical velocity obtained in this way agrees with that obtained by means of the complete linear stability analysis within 1% in the whole range of  $gn_0/E_R$  and  $V_{\max}$  considered in the present work. This confirms that the energetic instability in the periodic potential is driven by long-wavelength excitations, since the excitation energy of the sound mode is the smallest in this limit, as it occurs in the case of a single barrier. Equation (6) can be used also for unitary fermions, as we will see in Section IV.

In Fig. 1, we show the critical velocity in the case of the single rectangular barrier (top panel) and the periodic potential (bottom panel) for various values of  $L/\xi$ . In both cases, one clearly sees that the results of the GP equation approach the LDA prediction for  $L/\xi \gg 1$ , as expected. The way of approach is, however, different. In the case of the periodic potential,  $v_c$  exhibits a plateau for  $L/\xi \lesssim 1$  and small  $V_{\max}$ ; the plateau is instead absent in the case of the single barrier. The latter case is simpler, because the chemical potential and the excitation spectrum are fixed by the asymptotic density  $n_0$  only and are unaffected by the external potential. In the limit of weak and thin barriers, our GP results agree with the analytic expression  $v_c/c_s^{(0)} \simeq 1 - (3/4)(LV_{\max}/\xi gn_0)^{2/3}$  already derived in Ref. [21]; conversely, for thick barriers ( $L/\xi \gg 1$ ), the  $V_{\max} \rightarrow 0$  limit of the LDA expression (3) is  $v_c/c_s^{(0)} \simeq 1 - \sqrt{3/2}(V_{\max}/gn_0)^{1/2}$  [25]. All curves obtained from the GP equation for the single barrier have a curvature which lies in between these two limiting cases. Instead, the periodic potential extends over the whole system and, consequently, for a given average density  $n_0$ , a change of  $V_{\max}$  affects both  $\mu$  and the excitation spectrum in a way that depends also on the value of the healing length  $\xi$ . In particular, if  $\xi$  is larger than the lattice spacing and  $V_{\max}$  is not too large, the energy associated with quantum pressure, which is proportional to  $1/\xi^2$ , acts against local deformations of the order parameter and the latter remains almost unaffected by the modulation of the external potential. This is the regime of the plateau in Fig. 1. In terms of Eq. (6), this regime occurs when the left-hand-side is  $\simeq P/m$  and the right-hand-side is  $\simeq c_s^{(0)}$ , so that the critical quasi-momentum obeys the relation  $P_c/m = c_s^{(0)}$ , which is the usual Landau criterion for a uniform superfluid in the presence of

weak impurities (see Appendix B for more details). This regime ends when, by increasing  $V_{\max}$ , the sound velocity  $c_s$  in the lattice [i.e., the right-hand-side of Eq. (6) evaluated at  $P = 0$ ] becomes comparable or less than the maximum of the left-hand-side. Since, for small  $V_{\max}$ ,  $\mu$  is proportional to  $n_0$  and the maximum of the left-hand-side of Eq. (6) is of the order of  $q_B/m$ , the above condition is obtained for  $\mu \simeq E_R$ . When  $V_{\max}$  is further increased, the chemical potential  $\mu$  becomes larger than  $E_R$ , the density is forced to oscillate and  $v_c/c_s^{(0)}$  starts decreasing. The system eventually reaches a regime of weakly coupled superfluids separated by strong barriers. This regime will be discussed in Section V.

It is worth noticing that, for  $V_{\max} < 2gn_0$  [35], loops (“swallow tails”) appear in the Bloch band structure of the superfluid in the periodic potential as a consequence of the nonlinearity of the GP equation. These states and their stability have been deeply discussed in Ref. [32] and are accounted for in our calculations. The sets of points in the bottom panel of Fig. 1, which are closest to the LDA curve (i.e., for  $L/\xi = 10$  and  $V_{\max}/\mu_{j=0} < 0.9$ , or for  $L/\xi = 5$  and  $V_{\max}/\mu_{j=0} < 0.8$ ) fall into this regime: the critical velocity is determined by the energetic instability occurring along the swallow tails and the critical quasi-momentum is outside the first Brillouin zone,  $P_c > \hbar q_B$ . Our numerical results for  $P_c$  well agree with those of Ref. [32].

Finally, from the solution of the GP equation one can calculate the current(velocity)-phase relation of the superfluid flowing through a single potential barrier. Examples are given in the top panel of Fig. 3. The figure shows that, for  $L/\xi = 10$ , the results of the GP calculations are close to those in the LDA limit not only for the critical velocity (the maximum value of  $v$ ) but also for the shape of the curve on the left of the maximum (stable branch). On the right of the maximum (unstable branch) the GP theory still works, providing solitonic solutions which are instead not accessible to the hydrodynamic theory without dispersion. We note that, when approaching the maximum from the right, the amplitude of solitons predicted by the GP equations vanishes and the two, stable and unstable, branches merge together [21].

#### IV. BOGOLIUBOV-DE GENNES THEORY FOR UNITARY FERMIONS

A similar analysis can be done for a superfluid Fermi gas in the BCS-BEC crossover at zero temperature. A suitable approach consists in the numerical solution of the BdG equations for the fermionic quasiparticle amplitudes  $u_i$  and  $v_i$  [29],

$$\begin{pmatrix} H'(\mathbf{r}) & \Delta(\mathbf{r}) \\ \Delta^*(\mathbf{r}) & -H'(\mathbf{r}) \end{pmatrix} \begin{pmatrix} u_i(\mathbf{r}) \\ v_i(\mathbf{r}) \end{pmatrix} = \epsilon_i \begin{pmatrix} u_i(\mathbf{r}) \\ v_i(\mathbf{r}) \end{pmatrix}, \quad (7)$$

with  $H'(\mathbf{r}) = -\hbar^2 \nabla^2 / 2m + V_{\text{ext}} - \mu$ . These equations can be used to calculate the order parameter  $\Delta(\mathbf{r}) =$

$-g\sum_i u_i(\mathbf{r})v_i^*(\mathbf{r})$ , the chemical potential  $\mu$ , and the energy density  $e$ .

For a superfluid Fermi gas in the presence of a single rectangular barrier, the BdG equations have already been used by Spuntarelli *et al.* [11] to calculate the critical current in the case of  $Lk_F = 4$ . Their results at unitarity are shown in the top panel of Fig. 2 (dots) where they are compared with the LDA prediction (3). The figure shows that, for this value of  $Lk_F$ , the BdG results are indeed close to the LDA curve; in this regime, also for fermions, the critical velocity is mostly determined by the local depletion of the density where the potential is maximum. Concerning the LDA curve, we notice that in the  $V_{\max} \rightarrow 0$  limit one can easily obtain the analytic expression

$$v_c/c_s^{(0)} \simeq 1 - \sqrt{2} [V_{\max}/(1 + \beta)E_F]^{1/2}. \quad (8)$$

In the lower panel of Fig. 2 we instead show our BdG results for unitary fermions in a periodic potential for various values of  $Lk_F$ . These results are obtained by using Bloch functions and solving the BdG equations with the same self-consistent procedure of Ref. [36]. In particular, the energy density  $e(n_0, P)$  is calculated as in Eq. (8) of Ref. [36] (see also [37]). From the energy density we then obtain the critical quasi-momentum and velocity by means of Eq. (6).

A striking similarity emerges from Figs. 1 and 2, revealing that bosons and unitary fermions have a rather similar behavior. The rapid approach of the BdG results to the LDA curve for  $Lk_F > 1$  in the lattice is consistent with the case of a single barrier, as well as with the behavior of bosons in the corresponding regime,  $L/\xi > 1$ . Our BdG calculations, which include an analysis of the quasi-particle energy spectra, show that the role of fermionic pair-breaking excitations, not included in Eq. (6), is negligible at unitarity, except for small  $V_{\max}$  and for very low densities, such that  $Lk_F \ll 1$  [38]. These fermionic excitations are instead expected to become important on the BCS side of the BCS-BEC crossover [10, 11].

In the bottom panel of Fig. 3 we show the BdG results of Ref. [11] for the current(velocity)-phase relation of the unitary Fermi superfluid flowing through a single potential barrier. As in the case of bosons (top panels) one can see that, for  $Lk_F$  larger than 1, the BdG results are close to the LDA limit both for the shape of the stable branch and the height of the maximum.

## V. WEAKLY COUPLED SUPERFLUIDS

By increasing the height of the barriers, such that  $V_{\max} \gg \mu$ , the critical velocity decreases. In the LDA regime ( $L/\xi \gg 1$  or  $Lk_F \gg 1$ ) this decrease is fast because the superfluid density locally follows the shape of the external potential and rapidly vanishes under a barrier as soon as  $V_{\max}$  exceeds  $\mu$ . Conversely, when  $\xi$  is of order  $L$  or larger, the coupling between the superfluid

regions on the two sides of a barrier remains significant also for larger values of  $V_{\max}$ , leading to the physics of macroscopic tunneling and Josephson junctions in weakly coupled superfluids (for bosons, see for instance [39]).

In this regime, one finds the well-known characteristic sinusoidal current-phase relation, i.e.,  $j(\delta\phi) = j_c \sin(\delta\phi)$ , where  $\delta\phi$  is the phase difference of the superfluid order parameter across the barrier [40]. In the periodic lattice we recover the tight-binding expression for the energy density, which is given by  $e(n_0, P) = e(n_0, 0) + \delta_J[1 - \cos(\pi P/P_{\text{edge}})]$ . Here,  $P_{\text{edge}}$  is the quasi-momentum at the edge of the Brillouin zone, namely,  $P_{\text{edge}} = \hbar q_B$  for BECs of bosonic atoms and  $P_{\text{edge}} = \hbar q_B/2$  for superfluids of fermionic atoms. The quantity  $\delta_J = n_0 P_{\text{edge}}^2 / \pi^2 m^*$  corresponds to the half-width of the lowest Bloch band and is related to the tunneling energy associated with the Josephson current. The effective mass  $m^*$  is defined *via* the relation  $1/m^* = (1/n_0)\partial_P^2 e(n_0, P)|_{P=0}$  [4, 41].

A consequence of the sinusoidal shape of the energy density in the tight-binding limit is that the critical quasi-momentum approaches the value  $P_c = P_{\text{edge}}/2$  and the critical velocity takes the following simple dependence on the effective mass:

$$v_c = \frac{1}{\pi} \frac{P_{\text{edge}}}{m^*}. \quad (9)$$

When  $s = V_{\max}/E_R \gg 1$ , the critical velocity decreases according to  $m/m^* \propto \exp(-2\sqrt{s})$ . The values of  $v_c$  obtained from Eq. (9), with  $m^*$  extracted from the GP calculation of  $e(n_0, P)$ , are plotted in the lower panel of Fig. 1 (thinner black solid lines) for  $L/\xi = 1$  and 1.57 in the region of  $V_{\max}/\mu_{j=0} \gtrsim 2$ . The agreement with the results of the complete stability analysis is remarkable. A similar agreement is also obtained for unitary fermions, when  $e(n_0, P)$  is taken from the BdG calculations, as shown in the lower panel of Fig. 2.

## VI. FINAL REMARKS

In all panels of Figs. 1 and 2 one can distinguish three limiting cases: i) a regime of hydrodynamic flow in the local density approximation for large  $L/\xi$  (or  $Lk_F$ ), corresponding to the points close to the thick solid lines; ii) a regime of macroscopic flow through thin and weak barriers, where the LDA is not applicable, i.e., for  $L/\xi \lesssim 1$  (or  $Lk_F \lesssim 1$ ) and  $V_{\max}/\mu < 1$ ; iii) a regime of weakly coupled superfluids separated by thin and strong barriers, i.e., for  $L/\xi \lesssim 1$  (or  $Lk_F \lesssim 1$ ) but  $V_{\max}/\mu \gg 1$ .

Concerning bosons, the experiments performed in Ref. [42] with condensates in deep optical lattices fall into the third regime and were consistently interpreted in terms of the dynamics of a chain of Josephson junctions. An investigation of energetic and dynamical instabilities of bosons in shallow lattices was instead reported by the same group in Ref. [6], in a range of parameters corresponding to the second regime, namely where the critical velocity for the energetic instability is close to



the sound velocity of the uniform superfluid, as in the standard Landau criterion. In this experiment, as in the one of Ref. [5], a sharp determination of the Landau critical velocity was, however, hindered by the inhomogeneity of the trapped condensate.

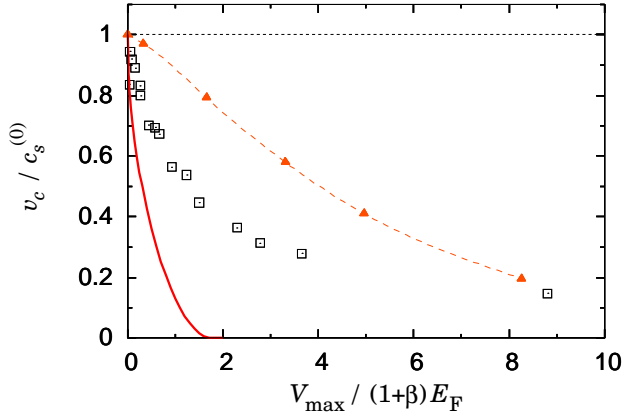


FIG. 4: (Color online) Comparison between theoretical results and the experimental data for the critical velocity of unitary fermions in an optical lattice. The filled triangles are our BdG results calculated for  $E_F/E_R = 0.5$ . The solid line is the prediction of hydrodynamics in LDA. The open squares are the experimental result of Ref. [7], normalized by using the density at the  $e^{-2}$  waist of the lattice, which corresponds to  $E_F/E_R = 0.56$ .

The critical velocity of fermions in an optical lattice is measured in Ref. [7]. The effects of the inhomogeneity of the density is reduced by producing the lattice in the central part of the atomic cloud. However, the lattice itself turns out to be inhomogeneous. This causes some uncertainties in the determination of both  $k_F$  and  $V_{\max}$ , which are needed for the comparison with a theory for a uniform superfluid in a uniform lattice. The waist of the two laser beams is smaller, but not much smaller than the Thomas-Fermi radii of the trapped gas. A reasonable choice consists of taking the density  $n_0$  as the density measured at the  $e^{-2}$  waist of the lattice, as suggested in Ref. [7]. This yields  $E_F/E_R \simeq 0.56$ , which means  $Lk_F \simeq 1.1$ . In Fig. 4 we show the experimental data (open squares) for this choice of  $k_F$ . Our BdG results for  $E_F/E_R = 0.5$  are shown as filled triangles, while the LDA result is represented by the thick solid line. Here  $v_c$  and  $V_{\max}$  are normalized to the sound velocity  $c_s^{(0)} = \sqrt{(1+\beta)/3} v_F$  and the chemical potential  $(1+\beta)E_F$  of the uniform gas, respectively [18]. The behavior of the experimental data significantly differs from the theoretical predictions. The disagreement remains qualitatively the same even for different choices of  $k_F$  and  $V_{\max}$  within the experimental uncertainties [43]. The failure of the LDA is expected, being consistent with the fact that here  $Lk_F$  is of the order of unity. The disagreement with the BdG calculations is instead puzzling, especially if one considers that most of the expected inaccuracy of

the BdG theory (e.g., the discrepancy between the mean-field result and the Monte-Carlo result of  $\beta$ ) is factorized out by the choice of the normalization in Fig. 4. This suggests that other effects, including the inhomogeneity of both the density and the lattice intensity, as well as the nonstationarity of the process, can be important in explaining the experimental observations. These effects could be better understood by repeating the same type of experiment with bosons, where the GP theory is reliable, full 3D GP simulations are feasible and a number of theoretical approaches are available to treat the case of time-dependent optical lattices (as, for instance, in Bragg spectroscopy experiments), from linear response theory to full nonlinear dynamics.

In view of the importance that energetic instabilities have in the description of superfluid phenomena, further experimental and theoretical investigations on the behavior of ultracold atomic superfluids in optical lattices and in the presence of obstacles are worth pursuing. An important step is the choice of a suitable geometry. Elongated systems with strong transverse confinement are good candidates, because their excitation spectrum is simpler. A new interesting perspective is also provided by the availability of toroidal confining potentials for ultracold gases [44, 45], in which one can produce a stationary superflow and explore the dissipation induced by an external perturbation along the torus [46].

## Acknowledgments

We acknowledge M. Modugno and A. Smerzi for fruitful discussions and for suggestions about the numerical techniques. Calculations were performed on the HPC facilities WIGLAF at the University of Trento, BEN at ECT\* in Trento, and RIKEN Super Combined Cluster System. This work, as a part of the European Science Foundation EUROCORES Program EuroQUAM-FerMix, is supported by funds from the CNR and the EC Sixth Framework Programme. It is also supported by MiUR.

## APPENDIX A: CRITICAL VELOCITY IN THE LDA HYDRODYNAMIC THEORY

In order to plot the LDA results in Figs. 1 and 2 we first rewrite Eq. (1) in terms of the velocity  $v_0 \equiv j/n_0$ . Its critical value,  $v_c$ , is determined by the condition that the local superfluid velocity  $v(z)$  coincides with the local sound velocity  $c_s(z)$  [Eq. (2)] at the position  $z = z_0$ , where the potential takes a maximum value  $V_{\text{ext}}(z_0) = V_{\max}$ . Using this condition,  $v(z_0) = c_s(z_0) = \sqrt{\alpha\gamma n^\gamma(z_0)/m}$ , together with the continuity equation,  $n(z_0)v(z_0) = n_0v_0$ , we write Eq. (1) as

$$\tilde{\mu}_c = \left(1 + \frac{2}{\gamma}\right) \left(\frac{\gamma}{2}\right)^{2/(\gamma+2)} \tilde{v}_c^{2\gamma/(\gamma+2)} + \tilde{V}_{\max}, \quad (\text{A1})$$

where  $\tilde{\mu}_c \equiv \mu_{j=0}/\alpha n_0^\gamma$ ,  $\tilde{v}_c^2 \equiv (mv_c^2/2)/\alpha n_0^\gamma$ , and  $\tilde{V}_{\max} \equiv V_{\max}/\alpha n_0^\gamma$ .

In the case of a single potential barrier, one finds  $\tilde{\mu}_c = \tilde{v}_c^2 + 1$ , so that Eq. (A1) becomes a third order algebraic equation for  $\tilde{v}_c^{2/3}$  when  $\gamma = 1$  (bosons), and a fourth order equation for  $\tilde{v}_c^{1/2}$  when  $\gamma = 2/3$  (unitary fermions). Once this algebraic equation is solved, one can use  $\mu_{j=0} = \alpha n_0^\gamma$  [i.e.,  $\mu_{j=0} = gn_0$  for bosons and  $\mu_{j=0} = (1 + \beta)E_F$  for unitary fermions] and plot  $v_c$  as a function of  $V_{\max}/\mu_{j=0}$ .

In the case of the periodic potential the procedure is similar, but the chemical potential must be calculated numerically for each value of the average density  $n_0$ . Equivalently, if  $z_1$  is a position where  $V_{\text{ext}}(z_1) = 0$ , one has  $\tilde{\mu}_c = \tilde{n}_1^{-2}\tilde{v}_c^2 + \tilde{n}_1^\gamma$ , with  $\tilde{n}_1 \equiv n(z_1)/n_0$ . We thus obtain an equation for  $\tilde{v}_c$  similar to the one of the single barrier, but where  $\tilde{n}_1$  has to be determined numerically. Using  $\mu_{j=0}$  obtained by a separate calculation, we can parametrically plot  $v_c$  as a function of  $V_{\max}/\mu_{j=0}$ .

## APPENDIX B: DETERMINATION OF THE CRITICAL QUASI-MOMENTUM IN A LATTICE

In this Appendix, we explain how we calculate the critical quasi-momentum  $P_c$  from the relation (6). As an example, in Fig. 5, we show the case of the unitary Fermi gas at  $E_F/E_R = 1$ , where  $P_c$  is in the first Brillouin zone [47]. Here, we drop the subscript “0” of the average density  $n_0$  for simplicity.

For the uniform case ( $s = 0$ ), the energy density can be written as  $e(n, P) = nP^2/2m + e(n, 0)$ , and thus  $\partial_n^2 e(n, P) = \partial_n^2 e(n, 0) = \partial_n \mu(n) = 1/(n\kappa)$  and  $\partial_P^2 e(n, P) = n/m$ . This implies

$$\sqrt{\frac{\partial^2 e}{\partial n^2} \frac{\partial^2 e}{\partial P^2}} = \sqrt{\frac{\kappa^{-1}}{m}} = c_s^{(0)}, \quad (\text{B1})$$

$$\frac{\partial^2 e}{\partial n \partial P} = \frac{P}{m}, \quad (\text{B2})$$

where  $\kappa$  is the compressibility and  $c_s^{(0)}$  is the sound velocity of the uniform system:  $c_s^{(0)} = \sqrt{(1 + \beta)/3} v_F$  ( $\simeq 0.44v_F$  from the mean-field theory, and  $\simeq 0.37v_F$  from Monte Carlo calculations) for unitary fermions and  $c_s^{(0)} = \sqrt{gn/m}$  for bosons. These results are shown as blue and red dashed lines in Fig. 5. Their crossing point,  $P/m = c_s^{(0)}$ , gives  $P_c$ . This procedure is consistent with the Landau criterion in a uniform gas.

For the superfluid in a lattice ( $s \neq 0$ ), since  $\partial_P e = 0$  at the edge of the Brillouin zone,  $\partial_n \partial_P e$  is zero there and has a maximum in the first Brillouin zone (see the red solid line in Fig. 5). For the same reason, there exists a new point  $P_{c, \text{dyn}}$  at which  $\partial_P^2 e = 0$  and the curve for  $\sqrt{\partial_n^2 e \partial_P^2 e}$  is bent downward (see the blue solid line in Fig. 5). This  $P_{c, \text{dyn}}$ , which does not exist for the uniform case, is the critical quasi-momentum for the dynamical instability of long-wavelength excitations; the excitation energy  $\hbar\omega$  becomes complex for  $P > P_{c, \text{dyn}}$ . The critical

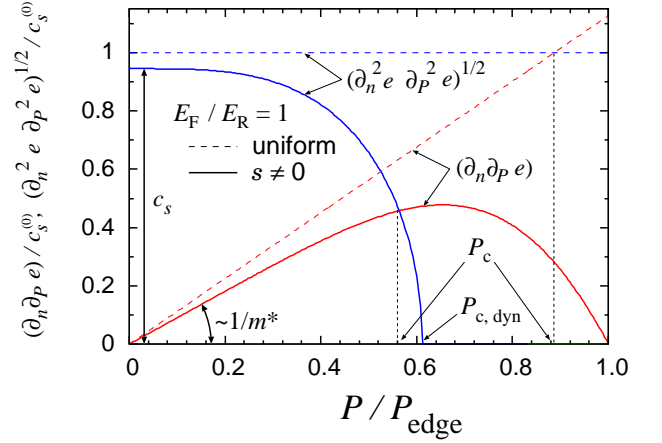


FIG. 5: (Color online) Schematic picture for the determination of the critical quasi-momentum  $P_c$  for the energetic instability using the hydrodynamic relation (6). Here we take the unitary Fermi gas at  $E_F/E_R = 1$  as an example. Dashed lines correspond to the uniform case ( $s = 0$ ) while solid lines to  $s = 1$ . The value of  $P_c$  is given by the abscissa of the crossing point between the curve representing  $\partial_n \partial_P e$  (red line) and  $(\partial_n^2 e \partial_P^2 e)^{1/2}$  (blue line). The critical quasi-momentum  $P_{c, \text{dyn}}$  for the dynamical instability of long-wavelength excitations is given by a zero of  $(\partial_n^2 e \partial_P^2 e)^{1/2}$ , where  $\partial_P^2 e = 0$ .

quasi-momentum for the energetic instability  $P_c$  is still given by the crossing point of  $\partial_n \partial_P e$  and  $\sqrt{\partial_n^2 e \partial_P^2 e}$  (red and blue lines) and thus  $P_c \leq P_{c, \text{dyn}}$ .

Note that the value of  $\sqrt{\partial_n^2 e \partial_P^2 e}$  (blue curve) at  $P = 0$  coincides with the sound velocity  $c_s$  in the lattice, which is decreasing function of  $s$  [48]. On the other hand the slope of  $\partial_n \partial_P e$  (red curve) is of order  $1/m^*$ , where  $m^*$  is the effective mass. Since  $c_s \propto 1/\sqrt{m^*}$  the slope of  $\partial_n \partial_P e$  approaches zero faster than  $c_s$  with increasing  $s$ . For large  $s$ , the red curve takes a sinusoidal shape and the crossing between the two lines occurs closer and closer to  $P = P_{\text{edge}}/2$ . In the same limit one finds  $P_c = P_{c, \text{dyn}}$ .

It is also worth noticing that, for both bosons and fermions in the lattice, there exists a value of average density  $n$  such that the critical momentum in the uniform case,  $mc_s^{(0)}$ , is equal to the critical quasi-momentum in the tight-binding limit,  $P_{\text{edge}}/2$ . In this case, we have numerically checked that  $P_c$  is almost independent of the lattice strength  $s$  in the whole range  $s \geq 0$ . With fermions, this condition occurs when  $E_F/E_R = (3/16)(1 + \beta)^{-1}$ ; for bosons, it occurs when  $gn_0/E_R = 1/\sqrt{2}$ . For smaller (larger) density, the critical quasi-momentum  $P_c$  is a monotonic function of  $s$  approaching the asymptotic value  $P_{\text{edge}}/2$  from below (above).



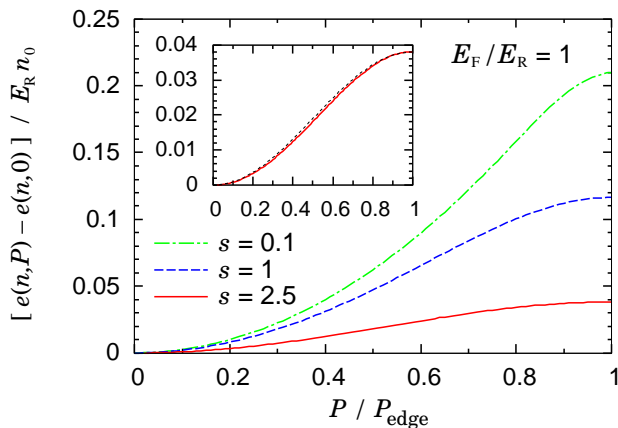


FIG. 6: (Color online) Energy density for fermions at unitarity as a function of the quasi-momentum  $P$  for various values of the lattice strength  $s$ . Here we take  $E_F/E_R = 1$  ( $k_F L = 1.57$ ) as an example. The inset shows the magnification of the result for  $s = 2.5$ ; the dotted line is a sinusoidal curve with the same amplitude.

### APPENDIX C: BAND STRUCTURE OF THE SUPERFLUID UNITARY FERMION GASES IN PERIODIC POTENTIALS

For superfluid Fermi gases in an optical lattice, solving the BdG equations with a large energy cutoff  $E_C$  is rather time-consuming. In the present work, in order to obtain the  $P$ -dependence of  $e$  and  $\mu$  for various parameters, we calculate them for a limited number of points (typically seven or more) in the first Brillouin zone for each  $E_F/E_R$

and we use the following fitting function:

$$f(n_0, P) = f(n_0, 0) + \delta(n_0) \left\{ \frac{1}{2} \left( 1 - \cos \left[ \pi \left( \frac{P}{P_{\text{edge}}} \right)^\eta \right] \right) \right\}^{1/\eta}, \quad (\text{C1})$$

with the band width,

$$\delta(n_0) \equiv f(n_0, P_{\text{edge}}) - f(n_0, 0). \quad (\text{C2})$$

The shape parameter  $\eta$  can take all values from 1 to  $\infty$ : the case  $\eta = 1$  corresponds to the sinusoidal form for strong lattices, while  $\eta = \infty$  reproduces the quadratic energy dispersion of the translationally invariant system without lattice ( $s = 0$ ). Note that  $\partial_P f(n_0, P) = 0$  at  $P = 0$  and  $P_{\text{edge}}$  like  $e$  and  $\mu$  (here, we do not consider situations where the band structure exhibits “swallow tails”). We find that the above fitting function (C1) very well reproduces the numerical BdG results of  $e$  and  $\mu$  except for the cases of very small  $s$ . Even for  $s = 0.1$ , which is the smallest non-zero value studied in the present work, the relative error is typically less than 0.1%.

In Fig. 6, we show the energy density  $e(n, P)$  of the unitary Fermi superfluid in a periodic potential calculated by the BdG equations for  $E_F/E_R = 1$  and for three values of the lattice strength,  $s = 0.1, 1$ , and  $2.5$ . The corresponding values of the shape parameter  $\eta$  are  $\eta = 5.05, 1.68$ , and  $1.13$ . Note that the  $P$ -dependence of  $e$  is rather close to a quadratic form for the weakest lattice ( $s = 0.1$ ) and is almost sinusoidal for the strongest lattice ( $s = 2.5$ ), as one can see in the inset of Fig. 6.

- 
- [1] L. D. Landau, J. Phys. USSR **5**, 71 (1941).
  - [2] P. Nozières and D. Pines, *The Theory of Quantum Liquids* (Perseus, Cambridge, 1999), Vol. II.
  - [3] C. J. Pethick and H. Smith, *Bose-Einstein Condensation in Dilute Gases 2nd ed.* (Cambridge Univ. Press, New York, 2008).
  - [4] L. P. Pitaevskii and S. Stringari, *Bose-Einstein Condensation* (Clarendon, Oxford, 2003).
  - [5] C. Raman, M. Köhl, R. Onofrio, D. S. Durfee, C. E. Kuklewicz, Z. Hadzibabic, and W. Ketterle, Phys. Rev. Lett. **83**, 2502 (1999).
  - [6] L. De Sarlo, L. Fallani, J. E. Lye, M. Modugno, R. Saers, C. Fort, and M. Inguscio, Phys. Rev. A **72**, 013603 (2005).
  - [7] D. E. Miller, J. K. Chin, C. A. Stan, Y. Liu, W. Setiawan, C. Sanner, and W. Ketterle, Phys. Rev. Lett. **99**, 070402 (2007).
  - [8] N. Andrenacci, P. Pieri, and G. C. Strinati, Phys. Rev. B **68**, 144507 (2003).
  - [9] R. Sensarma, M. Randeria, and T.-L. Ho, Phys. Rev. Lett. **96**, 090403 (2006).
  - [10] R. Combescot, M. Yu. Kagan, and S. Stringari, Phys. Rev. A **74**, 042717 (2006).
  - [11] A. Spuntarelli, P. Pieri, and G. C. Strinati, Phys. Rev. Lett. **99**, 040401 (2007).
  - [12] L. P. Pitaevskii, S. Stringari, and G. Orso, Phys. Rev. A **71**, 053602 (2005).
  - [13] A. A. Burkov and A. Paramekanti, Phys. Rev. Lett. **100**, 255301 (2008).
  - [14] F. Ancilotto, L. Salasnich, and F. Toigo, Phys. Rev. A **79**, 033627 (2009).
  - [15] Y. Yunomae, D. Yamamoto, I. Danshita, N. Yokoshi, and S. Tsuchiya, e-print arXiv:0904.3179.
  - [16] R. Ganesh, A. Paramekanti, and A. A. Burkov, Phys. Rev. A **80**, 043612 (2009).
  - [17] S. Giorgini, L. P. Pitaevskii, and S. Stringari, Rev. Mod. Phys. **80**, 1215 (2008).
  - [18] Ab-initio Monte Carlo simulations give  $\beta = -0.58 \pm 0.01$ . See J. Carlson, S.-Y. Chang, V. R. Pandharipande, and K. E. Schmidt, Phys. Rev. Lett. **91**, 050401 (2003); G. E. Astrakharchik, J. Boronat, J. Casulleras, and S. Giorgini, Phys. Rev. Lett. **93**, 200404 (2004); J. Carlson and S. Reddy, Phys. Rev. Lett. **95**, 060401 (2005). The value predicted by the BdG theory is instead  $\beta = -0.41$ . We use this value whenever we plot our BdG results for fermions. When theory is compared with experimental

- data, as in Fig. 4, we use  $\beta = -0.58$  for the latter.
- [19] We observe that, in the LDA hydrodynamic theory,  $n(z)$  and  $v(z)$  exhibit a kink at the point where  $v(z) = c_s(z)$ , with a finite jump in the first derivative, and one cannot construct a stationary solution for  $v(z) > c_s(z)$ .
  - [20] Yu. G. Mamaladze and O. D. Cheishvili, Zh. Eksp. Teor. Fiz. **50**, 169 (1966) [Sov. Phys. JETP **23**, 112 (1966)].
  - [21] V. Hakim, Phys. Rev. E **55**, 2835 (1997).
  - [22] P. Leboeuf, N. Pavloff, and S. Sinha, Phys. Rev. A **68**, 063608 (2003).
  - [23] Whenever the critical condition for Landau instability is reached at a position  $z_0$  far from the barrier edge, at a distance much larger than the healing length  $\xi$ , the results for the critical velocity are insensitive to the details of the shape of the barrier and are expected to be the same for both sharp and smooth barrier. In the LDA limit, this condition is satisfied and, indeed, our results for the rectangular barrier are consistent with the results discussed in Ref. [21] for a generic slowly varying potential. Of course, the LDA would not be reliable in predicting, for example, the behavior of the density distribution near the edge of the barrier, within a distance of order  $\xi$ .
  - [24] N. Pavloff, Phys. Rev. A **66**, 013610 (2002).
  - [25] A. M. Leszczyszyn, G. A. El, Yu. G. Gladush, and A. M. Kamchatnov, Phys. Rev. A **79**, 063608 (2009).
  - [26] E. P. Gross, Nuovo Cimento **20**, 454 (1961).
  - [27] L. P. Pitaevskii, Zh. Eksp. Teor. Fiz. **40**, 646 (1961) [Sov. Phys. JETP **13**, 451 (1961)].
  - [28] F. Dalfovo, S. Giorgini, L. Pitaevskii, and S. Stringari, Rev. Mod. Phys. **71**, 463 (1999).
  - [29] P. G. de Gennes, *Superconductivity of Metals and Alloys* (Benjamin, New York, 1966), Chap. 5, pp. 137-170.
  - [30] Given  $j$  and  $n_0$ , Eq. (4) admits two symmetric bounded stationary solutions which merge and disappear at the critical point  $j = j_c$ . These solutions can be expressed in terms of Jacobi elliptic functions [20] in which  $j$  and  $n_0$  enter as parameters. Upon matching the density derivative at the edge of the barrier, one is left with only one free parameter, to be in turn fixed by the matching of the density itself. The latter gives a non-algebraic equation, which we solve by means of a standard numerical root finding method.
  - [31] B. Wu and Q. Niu, Phys. Rev. A **64**, 061603(R) (2001).
  - [32] M. Machholm, C. J. Pethick, and H. Smith, Phys. Rev. A **67**, 053613 (2003).
  - [33] M. Modugno, C. Tozzo, and F. Dalfovo, Phys. Rev. A **70**, 043625 (2004).
  - [34] E. Taylor and E. Zaremba, Phys. Rev. A **68**, 053611 (2003).
  - [35] D. Diakonov, L. M. Jensen, C. J. Pethick, and H. Smith, Phys. Rev. A **66**, 013604 (2002).
  - [36] G. Watanabe, G. Orso, F. Dalfovo, L. P. Pitaevskii, and S. Stringari, Phys. Rev. A **78**, 063619 (2008); note that Eq. (8) of this paper contains a misprint: a factor  $(1/V)$  should be inserted on the right hand side in order to obtain the energy density.
  - [37] In order to cure the ultraviolet divergences in the BdG theory with contact potentials we use the regularization scheme proposed by G. Bruun, Y. Castin, R. Dum, and K. Burnett, Eur. Phys. J. D **7**, 433 (1999), and A. Bulgac and Y. Yu, Phys. Rev. Lett. **88**, 042504 (2002). We set the cutoff energy  $E_C = 50E_R$  for  $E_F/E_R < 0.5$  and  $E_C = 100E_F$  for  $E_F/E_R \geq 0.5$ .
  - [38] The creation of fermionic pair-breaking excitations under a barrier implies a transfer of momentum to the barrier of the order of  $\sim 2\hbar k_F$ . The probability of this process is expected to be proportional to  $\exp(-Lk_F)$  and hence to be negligible for large  $L$ .
  - [39] F. Dalfovo, L. Pitaevskii, and S. Stringari, Phys. Rev. A **54**, 4213 (1996); A. Smerzi, S. Fantoni, S. Giovanazzi, and S. R. Shenoy, Phys. Rev. Lett. **79**, 4950 (1997); I. Zapata, F. Sols, and A. J. Leggett, Phys. Rev. A **57**, R28 (1998); S. Giovanazzi, A. Smerzi, and S. Fantoni, Phys. Rev. Lett. **84**, 4521 (2000); F. Meier and W. Zwerger, Phys. Rev. A **64**, 033610 (2001).
  - [40] An analytic derivation of the current-phase relation for bosons in the presence of a thin barrier is given, for instance, in I. Danshita, N. Yokoshi, and S. Kurihara, New J. Phys. **8**, 44 (2006).
  - [41] M. Krämer, C. Menotti, L. Pitaevskii, and S. Stringari, Eur. Phys. J. D **27**, 247 (2003).
  - [42] F. S. Cataliotti, S. Burger, C. Fort, P. Maddaloni, F. Minardi, A. Trombettoni, A. Smerzi, and M. Inguscio, Science **293**, 843 (2001).
  - [43] In Fig. 4, we use the same lattice height used in Ref. [7], which is characterized by the peak value over the sample. If we use the lattice height at the  $e^{-2}$  waist instead,  $V_{\max}$  of both the experimental data (open squares) and our theoretical prediction (filled squares) will be reduced by the same factor and thus the discrepancy still remains.
  - [44] C. Ryu, M. F. Andersen, P. Cladé, V. Natarajan, K. Helmerson, and W. D. Phillips, Phys. Rev. Lett. **99**, 260401 (2007).
  - [45] S. Franke-Arnold, J. Leach, M. J. Padgett, V. E. Lembessis, D. Ellinas, A. J. Wright, J. M. Girkin, P. Ohberg, and A. S. Arnold, Optics Express **15**, 8619 (2007).
  - [46] See, for instance, F. Piazza, L.A. Collins, and A. Smerzi, Phys. Rev. A **80**, 021601(R) (2009) and references therein.
  - [47] In general, there are also cases where  $P_c$  is outside the first Brillouin zone, as we have seen for bosons when the energy exhibits swallow tails. In Appendix B, we do not consider this case for simplicity, but the procedure for calculating  $P_c$  is the same.
  - [48] Note that in this work we always consider a flow along the direction of the 1D lattice. It is worth noticing here that the critical velocity of the superfluid flowing instead along the transverse direction can be larger than the sound velocity for the uniform system  $c_s^{(0)}$ . In fact, since the system is translationally invariant in the transverse direction, one has  $m^* = m$ ,  $\partial_n \partial_{P_\perp} e = P_\perp/m$ , and  $\kappa$  does not depend on the transverse momentum  $P_\perp$ . On the other hand, due to the periodic potential,  $\kappa^{-1}$  can be larger than that of the uniform system with the same average density [36, 41]. Under these conditions, both the sound velocity in the lattice and the critical velocity,  $v_c = \sqrt{\partial_n^2 e \partial_{P_\perp}^2 e} = \sqrt{\kappa^{-1}/m}$ , are larger than  $c_s^{(0)}$ .